Available online at www.sciencedirect.com

ScienceDirect

journal homepage: www.elsevier.com/locate/he

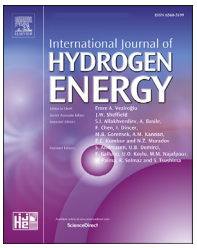

Synthesis of activated ferrosilicon-based microcomposites by ball milling and their hydrogen generation properties

Paul Brack [a], *S.E. Dann* [a,*], *K.G.U. Wijayantha* [a], *Paul Adcock* [b], *Simon Foster* [b]

[a] *Department of Chemistry, Loughborough University, Loughborough, Leicestershire, LE11 3TU, United Kingdom*
[b] *Intelligent Energy Ltd, Charnwood Building, Holywell Park, Ashby Road, Loughborough, Leicestershire LE11 3GB, United Kingdom*

ARTICLE INFO

Article history:
Received 15 October 2017
Received in revised form
13 November 2018
Accepted 4 December 2018
Available online 4 January 2019

Keywords:
Ball-milling
Ferrosilicon
Hydrogen generation
Hydrolysis
Additives

ABSTRACT

Ferrosilicon 75, a 50:50 mixture of silicon and iron disilicide, has been activated toward hydrogen generation by processing using ball milling, allowing a much lower concentration of sodium hydroxide (2 wt%) to be used to generate hydrogen from the silicon in ferrosilicon with a shorter induction time than has been reported previously. An activation energy of 62 kJ/mol was determined for the reaction of ball-milled ferrosilicon powder with sodium hydroxide solution, which is around 30 kJ/mol lower than that previously reported for unmilled ferrosilicon. A series of composite powders were also prepared by ball milling ferrosilicon with various additives in order to improve the hydrogen generation properties from ferrosilicon 75 and attempt to activate the silicon in the passivating $FeSi_2$ component. Three different classes of additives were employed: salts, polymers and sugars. The effects of these additives on hydrogen generation from the reaction of ferrosilicon with 2 wt% aqueous sodium hydroxide were investigated. It was found that composites formed of ferrosilicon and sodium chloride, potassium chloride, sodium polyacrylate, sodium polystyrene sulfonate-co-maleic acid or fructose showed reduced induction times for hydrogen generation compared to that observed for ferrosilicon alone, and all but fructose also led to an increase in the maximum hydrogen generation rate. In light of its low cost and toxicity and beneficial effects, sodium chloride is considered to be the most effective of these additives for activating the silicon in ferrosilicon toward hydrogen generation. Materials characterisation showed that neither ball milling on its own nor use of additives was successful in activating the $FeSi_2$ component of ferrosilicon for hydrogen generation and the improvement in rate and shortening of the induction period was attributed to the silicon component of the mixture alone The gravimetric storage capacity for hydrogen in ferrosilicon 75 is therefore maintained at only 3.5% rather than the 10.5% ideally expected for a material containing 75% silicon. In light of these results, ferrosilicon 75 does not appear a good candidate for hydrogen production in portable applications.

* *Corresponding author.*
E-mail address: S.E.Dann@lboro.ac.uk (S.E. Dann).

https://doi.org/10.1016/j.ijhydene.2018.12.008

Introduction

Hydrogen generation for portable fuel cell devices

In recent years, the explosion in the use of portable electronic devices has driven an increase in demand for systems which can produce electricity on the move [1–4]. One of the most promising methods to generate electricity in a portable device is to use proton exchange membrane (PEM) fuel cells [5–11]. These possess two major advantages over batteries: first, PEM fuel cells have a greater power density than batteries, and second, PEM fuel cells will continue to generate electricity as long as they are fed with hydrogen, allowing them to operate for a longer time than batteries [12,13]. However, these advantages are only realisable if appropriate portable sources of hydrogen can be developed.

Portable devices need to be recharged regularly by their users and as a result this limits the method of hydrogen generation to materials which can store hydrogen and release it predictably and on demand. Although hydrogen gas may seem an attractive choice of fuel due to its high energy density by weight and an environmentally friendly combustion product; H_2O. the low liquefaction temperature (20.3 K) and the need for heavy walled pressurised storage tanks are impractical for mobile application use [14,15]. Alternative options are hydrogen storage materials that fall into two categories which generate hydrogen by either thermolysis or hydrolysis. For portable applications, thermolysis of metal hydrides is not favoured as methods of heating/cooling safely must be built into the device to make it operate; this acts to increase the bulk of the device which is limited by the requirement to be transportable. Light elements which generate hydrogen by a hydrolysis reaction are therefore more favoured, since they can produce a high percentage of hydrogen per unit mass. These materials are considered to store the hydrogen in the water that they react with rather than in the metal itself. In some cases this reaction is too violent to be viable for portable application e.g. in the case of sodium, but in other examples, the formation of a passivating oxide layer allows the high gravimetric storage capacity of silicon (14%) and aluminium (11%) to be transported and utilised when required [16–26].

Hydrogen generation from silicon

Silicon has a high natural abundance, making up ca. 27% of the Earth's crust, largely in the form of silicates including quartz and feldspars [27]. Silicon has attracted considerable interest in recent years due to its theoretically simple reaction with water (Equation (1)) which is accompanied by a high standard enthalpy change for the reaction (−409 kJ mol-1)[28] as well as the production of hydrogen.

$$Si(s) + 2H_2O \rightarrow 2H_2(g) + SiO_2(s) \quad (1)$$

The rise in industrial demand for silicon has been more recent [19] than for aluminium, with the majority of its uses in high value applications. Silicon is used in vast quantities for e.g producing semiconducting silicon wafers which typically must be produced in high purity for optimal performance e.g solar grade products. Although this could be considered a concern and possibly a competing area of demand for silicon against that for its utilisation in hydrogen production, it also means there is growing interest in processing and recycling silicon waste. Porous silicon has been generated from electrochemical etching of p-type wafers for hydrogen storage [29] and nanosilicon has been tested in nanoemulsions in internal combustion engines to create hydrogen in-situ [30].

Under standard conditions, water on its own it not normally sufficient to release hydrogen from silicon due to the previously discussed passivating oxide layer. While the oxide layer is useful in generating a material which can be safely transported, it does not contribute to the generation of hydrogen itself and acts to retard its release from the underlying metal. This can be considered as a blocking effect where the oxide prevents the reaction of the solution with the metal that is covered by the protecting layer. As a result, an activation process is typically undertaken to remove the oxide and access the metal and its associated stored hydrogen via reaction with water. A variety of methods exist to accelerate the penetration of the solution through the oxide layer and/or limit its thickness. The first of those is to use a strong acid or base as an etchant to chemically remove the oxide layer and allow attack of the reaction solution on the light element. Hu [31] released hydrogen from waste silicon wafers using strong base while Zhan and coworkers [32] used base and a magnesium alloy to form silicon oxide hydride from porous silica. Kao improved the release of hydrogen by base catalysis of kerf loss silicon by using additives including sodium metasilicate and silicic acid [33]. Erogbogbo, also used an ingenious laser pyrolysis method to reduce the oxide layer in nanosilicon [34] while Goller investigated the effect of pH on the nanosilicon/water reaction [35]. High concentrations of acid/base are very effective at removing the oxide but are less desirable from a portable application point of view, both from a safety of the user perspective and possible damage to the container in which the device is housed. The literature has thus shown a particular focus on reducing the acid/base concentration and/or developing materials which can react with water alone. The second method for removal of the oxide layer involves thinning/damaging of the oxide layer by abrasion. This can be achieved in many different ways from simple hand grinding in a pestle and mortar to ball milling. An additional advantage of using the ball milling methodology is that the particle size also tends to be reduced, leading to increased defects/grain boundaries and hence enhanced reaction rates. Grain boundaries are thought to retard oxide layer build up and allow the oxide layer to be more easily breached.

Ferrosilicon; a cheap hydrogen generating silicon/iron disilicide composite

Ferrosilicon is a low cost material prepared by reducing the waste from the processing of iron oxide ore with coke leading to a mixture of iron, silicon and/or iron silicide phases depending on the iron:silicon ratio [36]. The most widely produced of these is ferrosilicon 75, where the 75 refers to a silicon content of ca. 75%, which is a 50:50 mixture of Si to $FeSi_2$ that has been used to produce hydrogen for over a

century. Unlike pure silicon, which has not been used in large scale applications to produce hydrogen, ferrosilicon was used on a massive scale to create hydrogen and power Zeppelins during World War I [37]. It is easy to transport and safe to handle by untrained personnel, only releasing hydrogen when treated with strong base. It therefore has the potential to be used in mobile applications due to a good safety record in the field, but only if the full potential of the silicon within it can be unlocked and the concentration of the base needed to release hydrogen (40% wt. NaOH) can be reduced. The theoretical gravimetric storage density of ferrosilicon 75 is 10.5% or ca. 75% of that of pure silicon on its own (14%), based on the ratio of silicon to iron in ferrosilicon 75 of 3:1; although this is similar to aluminium (11%), ferrosilicon 75 is a much cheaper commodity as it is prepared from mining waste [36]. However the full hydrogen generation capability of the mixture cannot be accessed, as two thirds of the silicon within the ferrosilicon is present in $FeSi_2$. $FeSi_2$ is an inert component which protects the active silicon from oxidation, acting as a passivating species in the similar way that a surface layer of silicon oxide passivates silicon metal. This composition means that the hydrogen generation behaviour of ferrosilicon is markedly different to silicon on its own. The role of spectator ($FeSi_2$) and active species (Si) in this material was confirmed in our laboratories [38] by experiment and showed that the gravimetric storage density for hydrogen of ferrosilicon 75 is only 3.5%; roughly a third of that expected for ferrosilicon 75 (10.5%) based on the silicon to iron ratio of 3:1 as most of the silicon is contained within the $FeSi_2$ and unavailable to produce hydrogen. Ways to attain the theoretical gravimetric storage density of 10.5% would be of great interest in mobile applications and/or back up power generation, as ferrosilicon 75 would be cheap to produce, easy to transport and safe to use.

While the very broad and complex area of metal corrosion is not required for the understanding of the hydrogen generation process in ferrosilicon, pitting corrosion is of interest as it describes how protecting layers such as oxide and/or intermetallics are disrupted by surface etchants. Pitting corrosion arises when a corrosive species penetrates through irregularities in the passivating oxide layer or intermetallic (such as $FeSi_2$) until it reaches the reactive metal interface. The presence of the anion at the surface leads to thinning and rupture of the passivating layer and creates a pit. As pits grow with further etchant anions attacking the same area, the concomitant hydrogen generation reaction is accelerated. Chloride is an anion which is well known for causing the pitting corrosion mechanism in both steel and aluminium. Alloying is an effective way of reducing the formation of oxide and the high stability of ferrosilicon is due the presence of $FeSi_2$ which allows ferrosilicon to be stored under ambient conditions without loss of reactivity. In the case of Al/Mg, alloying with more electropositive metals acts to enhance hydrogen production through galvanic corrosion, but for $FeSi_2$ this is not the case and it remains inert throughout the reaction of ferrosilicon with base. The resistance of $FeSi_2$ to corrosion also results in a significant induction time to produce the hydrogen which is not ideal from a portable application perspective. Rate of hydrogen production is also very slow unless high concentrations of base are used, typically 40% wt. Sodium hydroxide, and a much lower concentration would be needed to utilise this reaction in a device due to health and safety considerations. Both these issues need to be addressed to use ferrosilicon practically.

Ball milling of hydrogen storage materials

Particle size reduction by ball milling is a process which is being used increasingly often to enhance the activity of chemical hydrogen storage materials, partly due to its potential scalability [39]. This has included standard ball milling of light metals pertinent to this study and more intricate versions of the technique such as employing dielectric-barrier discharge plasma [40] ball-milling on metal hydrides [41] such as MgH_2. Alinejad and Mahmoodi used the standard ball-milling method to obtain induction-period free hydrogen generation by reaction of a NaCl:Al composite with pure water [42]. Czech and Troczynski [43] and Swamy and Shafirovich [44] have reported slightly contradictory results on the effects of leaching out the sodium chloride by dissolution in cold water before reaction to generate hydrogen. Czech and Troczynski found that the leached-out powders reacted in the same way as the composite powders (in terms of induction periods and hydrogen yields), whereas Swamy and Shafirovich found that leached out powders showed longer induction periods than composite powders; they ascribe this change to surface passivation engendered by the formation of an oxide layer during the drying stage after leaching (the powders were dried in air overnight). The authors found that the primary cause of the activation of the aluminium powders is the production of grain boundaries, dislocations and inclusions in the oxide layer and the exposure of fresh aluminium surface by the deformation of the aluminium. Foord et al. demonstrated the use of several additives, notably sodium polyacrylate, sucrose and sodium chloride, in the activation of silicon to generate hydrogen with water [45,46]. Their explanation of the mechanism of action of the additives was as follows. When the composite powder is exposed to water, the highly water soluble dispersants, termed dispersing agents, such as sodium chloride and sucrose rapidly leach out of the composite powder into solution, which in turn promotes the dispersion of the silicon particles and increases their exposed surface area and thus their availability for reaction. These authors found that sodium chloride caused agglomeration of silicon particles, while sucrose was found to decrease agglomeration with respect to the powder milled without additives. This led to rapid initial reactions with sodium chloride-silicon composites before a drop in rate and a lengthier reaction time due to the aggregation of silicon onto the surface of the silicon particles, blocking the reaction. When sucrose was just added to solution, it was found to cause a decrease in the reaction rate such that it was lower than when there was no additive; this indicated that it was the leaching out process that was critical to the activation.

Foord et al. also studied the use of polyelectrolytes as colloidal stabilisers [45,46]. They found that the addition of anionic polyelectrolytes, and in particular, sodium polyacrylate to an aqueous solution was sufficient to double the rate of hydrogen generation with respect to the reaction in cold water. The authors also found that the stability of the colloid increased as more PAA was added to solution; this led

to a larger reactive surface area (of the silicon) and a faster reaction.

Activation of ferrosilicon for mobile applications

In this work, we seek to activate ferrosilicon 75, a 50:50 mixture of silicon and $FeSi_2$, which was used to generate hydrogen for airships in the early 20th century [37], by ball milling with various additives in a similar way to that described for silicon and aluminium. Ferrosilicon is a cheap, low-toxicity material which is readily available on the multi-tonne scale. In previous work, we have demonstrated that ferrosilicon 75 generates hydrogen by the reaction of its metallic silicon component with sodium hydroxide solution [38]. However, induction periods were lengthy and reaction rates sluggish unless a high concentration (40 wt%) of sodium hydroxide solution was deployed to etch the surface chemically [38,47]. As well as retarding the release of hydrogen from silicon, the $FeSi_2$ component in ferrosilicon was also shown to be unchanged during the hydrogen generation process, meaning there is potential to unlock further silicon for hydrogen generation from the composite. Though the ball milling of ferrosilicon to obtain silicon for lithium-ion battery applications has recently been reported [48,49], to our knowledge no studies exist on the application of ball-milling ferrosilicon and ferrosilicon composite powders for hydrogen generation. This paper examines the effects of milling and additives on ferrosilicon 75 and their ability to activate in the presence of base the two components in the system, Si and $FeSi_2$, for hydrogen release.

Material and methods

Synthesis and characterisation methods

Ferrosilicon 75 was purchased from Castree Kilns. LCMS-grade acetonitrile, sodium hydroxide, sodium polyacrylate (PAA, MW 5100), sucrose, fructose, lactose monohydrate, glucose, mannose, poly (sodium 4-styrenesulfonate) (PSS, MW ~70000), polyethylene glycol (PEG, MW ~10000), polyvinylalcohol (PVA, MW ~89000–98000), poly (4-styrenesulfonic acid-co-maleic acid) sodium salt (PSScoMA, MW ~20000), potassium chloride and sodium chloride were purchased from Sigma Aldrich. All chemicals were used as received.

Ball milling was carried out using a Fritsch Pulverisette 6 ball mill equipped with an 80-mL tempered steel bowl and tempered steel balls (5 mm diameter, 130 g). In the milling experiments, 6.5 g of ferrosilicon powder was placed in the bowl along with the balls, acetonitrile (15 mL) and the appropriate amount of additives (polymers: 1.3 g; sugars and salts: 3.25 g) and this was then placed in the ball mill and milled at a 600 rpm for 15 min, unless otherwise stated. Once the milling process was finished, the bowl was left to cool, after which time the solid material still suspended in acetonitrile was extracted with a plastic pipette and transferred to a sample vial to dry in air. The balls and bowl from the ball mill were then washed with acetonitrile several times to recover any residual product left on the bowl or balls of the mill, and the washings were also transferred to the sample vial. The sample was then left to dry with no heating by evaporation of the solvent in air. The ball milled powdered samples were then stored in ambient air before being using to generate hydrogen.

Powder X-ray diffraction data were collected in transmission geometry on a Bruker D8 Discover diffractometer using Co Kα1 radiation and a Braun linear position sensitive detector over the 2θ range 15–95° with a step size of 0.007° 2θ and a count time of 1.0 s per step. FTIR spectra were obtained using a Shimadzu IR Affinity-1 FTIR spectrometer with a Specac ATR Sampling Accessory.

X-ray photoelectron spectroscopy (XPS) studies were conducted using a VG Scientific Escalab Mk I instrument operating with a monochromatic Al Kα X-ray source (1486.6 eV). The powders were imaged using a Leo 1530 VP field emission gun scanning electron microscope (FEG-SEM) at an accelerating voltage of 5 kV. Particle size distributions based on SEM images were obtained using Zeiss' software package AxioVision SE64 (Release 4.9.1). Elemental maps were generated by energy Dispersive X-ray (EDX) spectroscopy, which was conducted using a Leo 1530 VP FEG-SEM at an accelerating voltage of 20 kV and a working distance of 8.5 mm. Particle size analyses and zeta potential measurements were conducted using a Zetasizer Nano (Malvern Instruments Ltd.).

Thermogravimetric analysis (TGA) was conducted using an SDT Q600 Thermal Analyser (TA Instruments) using a ramp rate of 10 °C/min up to 700 °C. Elemental analysis was conducted using a CE-440 Elemental Analyser (Exeter Analytical, Inc.).

Procedure for determining hydrogen production

The reactions between both ball-milled ferrosilicon and ferrosilicon composite powders produced by ball-milling with sodium hydroxide were then investigated. 5 mL of 2 wt% sodium hydroxide solution (unless otherwise stated) was added to a 50-mL round bottomed flask and left to equilibrate to the desired temperature (typically 55 °C) for 10 min. In the case of ball milled ferrosilicon, 0.2 g of the solid was added to the sodium hydroxide solution in the flask and the volume of hydrogen evolved was recorded using the water displacement method previously described elsewhere [50]. over a period of time long enough to ensure no more hydrogen was being produced (typically 10 min). The analogous experiment for the ball milled ferrosilicon composite mixtures was carried out in the same way, except the amount of solid added was adjusted to take account of the additive and keep the mass of ferrosilicon constant at 0.2 g. This was 0.3 g of salt/sugar ball-milled ferrosilicon composite and 0.24 g of polymer ball-milled ferrosilicon composite respectively.

Results and discussion

Characterisation of ferrosilicon starting material (without additives)

The as received (unmilled) ferrosilicon 75 starting material was first characterised using physical characterisation techniques (XRD, XPS) to investigate particle size and identify the

phases present. A hydrogen generation profile for this material was then produced to generate a standard profile for the material where no treatment (milling or addition of additives) had taken place. After this initial characterisation, milled ferrosilicon was prepared from this standard with no additives present to investigate the effect of milling on the hydrogen generation profile. These data were collected to provide comparative data for the additive experiments carried out in sections 3.2.

Characterisation of as-received ferrosilicon powders

The characterisation of the ferrosilicon 75 starting material used in this study has been described previously [38]. It was found that the material consisted predominantly of inhomogenously distributed crystalline phases of silicon and iron disilicide, with a silicon rich surface. Representative data are included in the Supporting Information (Figs. S1-S3). The powders were found to have a mean particle size of 51.2 μm with a standard deviation of 39.9 μm, highlighting the very inhomogeneous nature of the particle size in this material. The non-homogeneity of the samples is unsurprising considering the fact that ferrosilicon is an industrial material prepared from reduction of iron oxide waste (from mining) with coke at high temperature rather than a fine chemical prepared from pure materials of well defined composition.

Hydrogen generation profiles from ferrosilicon 75 using sodium hydroxide have also been described previously [38,47]. The poor homogeneity and large particle size present in this material means that concentrated sodium hydroxide (40% wt) is needed to generate hydrogen otherwise very lengthy induction periods are observed before any hydrogen is released. The first stage in trying to shorten the induction period and increase the rate of reaction, was through ball milling the material on its own with no additives. .

Materials characterisation of ferrosilicon powders following ball-milling

In an effort to achieve the smallest possible particle sizes within the limitations of the equipment available, balls of small diameter (5 mm) and the highest rotation speed of the ball mill (600 rpm) were utilised. A short milling period (15 min) was used in order to avoid problems of forming large agglomerates or of reoxidising the surface of the powder [22]. The milled powder was characterised using PXRD, ATR-FTIR, XPS, TGA, SEM-EDX and DLS. The PXRD pattern confirmed that no phase changes occurred during the ball milling process and no new phases were formed; some impurity phases may still be present that cannot be detected by X-ray diffraction either by being too poorly crystalline and/or in too lower concentration. The positions of the reflections are noted in the figure with a # for Si and a * for $FeSi_2$. Analysis by ATR-FTIR and TGA (as there was very little weight loss) suggested that there was very little acetonitrile remaining in the powders after the simple drying process of standing the ground material in air and allowing the acetonitrile to evaporate. This was further confirmed by XPS analysis, which indicated the presence of 4 at.% N at the surface. High resolution XPS spectra of the Si 2p region before and after milling (Fig. 1(a)) suggest that there is an increase in the intensity of the peak which is primarily indicative of silicon (99.1 eV) with respect to the peak corresponding to silicon dioxide (103.1 eV), indicating that the milling process effectively decreases the thickness of the

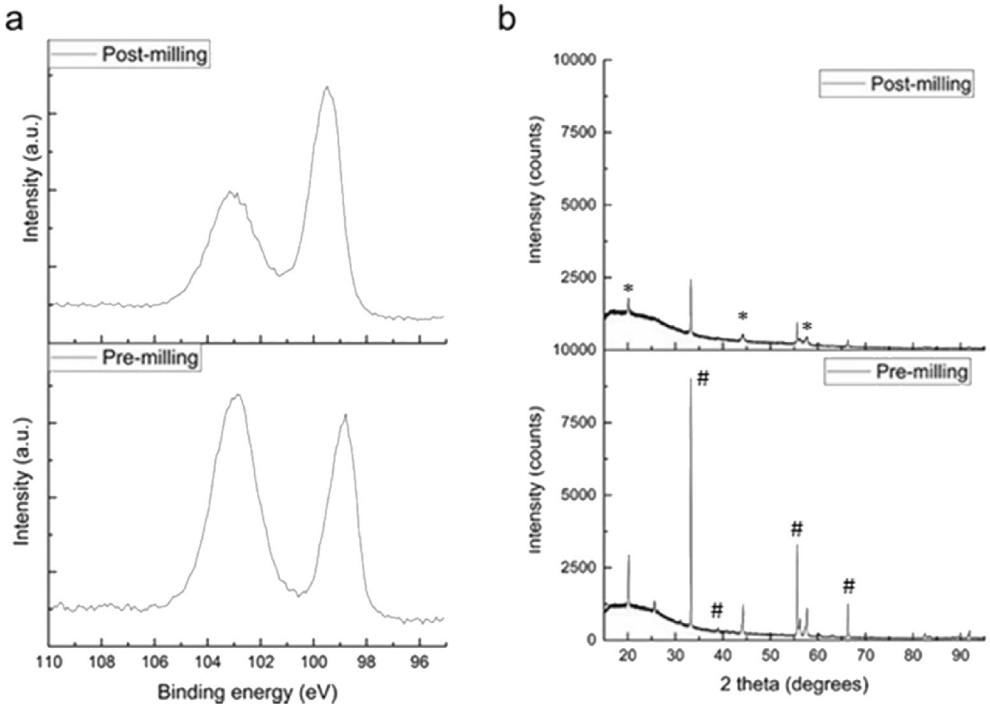

Fig. 1 – a) XPS spectra of the Si 2p region for pre- and post-milled ferrosilicon 75 powders. b) PXRD pattern of ferrosilicon 75 before (bottom) and after (top) ball milling. Reflections corresponding to silicon are indicated by #, while major reflections corresponding to iron disilicide are indicated by *.

surface oxide layer. The PXRD patterns (Fig. 1(b)) of the powders before and after milling show that there is no change in the crystalline phase composition of the material during the milling process with only silicon reflections (denoted by a #) and iron disilicide reflections denoted by a *) present in the pattern. The lower intensity and broader reflections are indicative of a smaller crystallite size after milling (according to the Debye-Scherrer equation where particle size is inversely proportional to full width at half maximum height of the reflections). A full Debye Scherrer analysis to determine the size reduction was not carried out due to the multiphase nature of ferrosilicon and the simplicity of the crystal system leading to few reflections.

SEM images of the powder after milling clearly show that the particle size is greatly reduced through the milling process (Fig. S1 and Fig. 2). It is also clear from the SEM images that the particle sizes are still fairly inhomogeneous, ranging from a few hundred nanometres to around a micron in at least one dimension, which is commonly observed in powders produced by ball milling [35,44]. An attempt to measure the particle size in suspension was made using dynamic light scattering (DLS). First, a sample of the powder was added to distilled water and then left to equilibrate. However, some particles settled (a Zeta potential of 3.06±0.14 mV at pH 7 was measured for the ball-milled ferrosilicon powder, confirming that it does not form a stable suspension); the average particle size of the suspended particles was found to be 370±11 nm. Agglomerates were also observed.

As described in section 1.3, the role of $FeSi_2$ in ferrosilicon is as a protector species for the active Si particles to prevent their surface oxidation and hence allows ferrosilicon to be easily packaged and transported; it is transported in barrels and no inert gas backfill is necessary as might be expected for silicon on its own. Iron disilicide remains inert throughout the hydrogen production process while the silicon is oxidised and hydrogen is produced. One of the goals of milling the ferrosilicon powder was to obviate the physical iron disilicide obstruction to the reaction of silicon with aqueous sodium hydroxide to improve the hydrogen generation properties of the bulk. The elemental distribution before and after milling was thus examined by energy dispersive X-ray spectroscopy (EDX). As shown in previous work [38] and reported in the literature [51], ferrosilicon alloys contain an inhomogeneous mixture of phases, and elemental maps of as-received ferrosilicon obtained by EDX clearly show discrete regions of silicon and iron disilicide (Fig. 3). After milling, the distribution of the relevant elements is far more even, indicating that the grain sizes of the individual phases are greatly reduced (Fig. 3). This decrease in grain size and presumed concomitant increase in the number of grain boundaries, defects and vacancies is expected to lead to activation of the powders towards hydrogen generation as it breaks down the inert $FeSi_2$ into smaller particles meaning the surface of the silicon is more exposed. Grinding also facilitates the breakdown of any oxide on the surface of the active silicon particles, in addition to the enhancement in rate obtained due to the reduction in particle size [39,52–54].

Hydrogen generation from ball-milled ferrosilicon powders

The hydrogen generation properties of the ball-milled ferrosilicon powders were investigated. Whereas in previous studies described in section 3.1.1, 40 wt% NaOH solutions were required to attain short induction times and reasonable rates

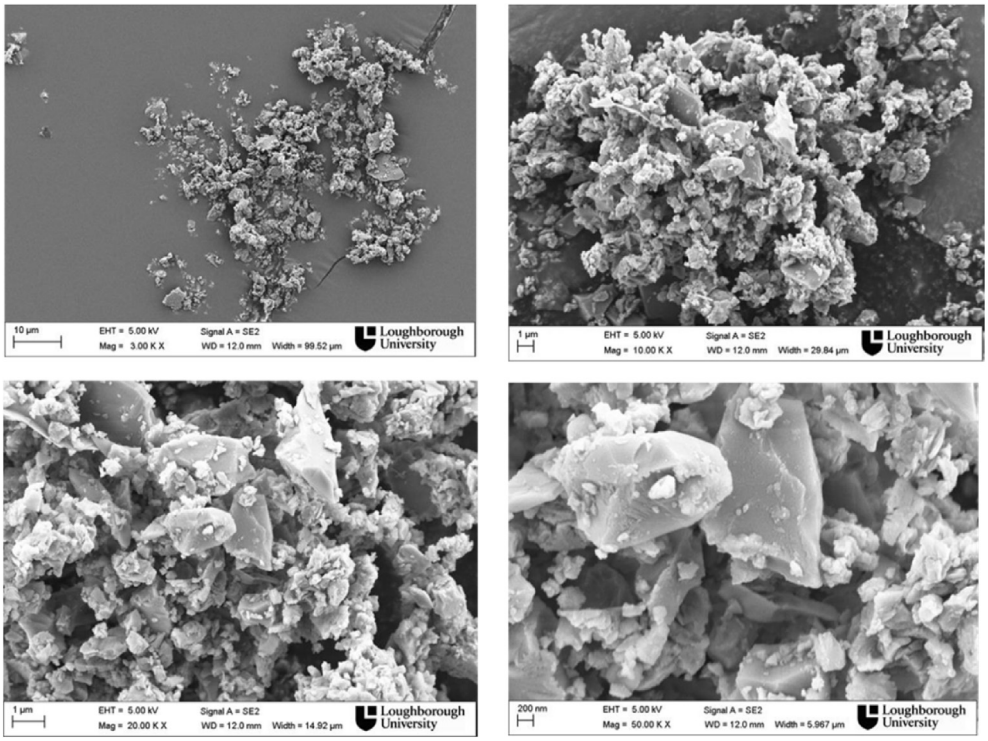

Fig. 2 – SEM images of ball-milled ferrosilicon 75 powder using different magnifications; top left 3x, top right, 10 x, bottom left 20 times and bottom right 50x.

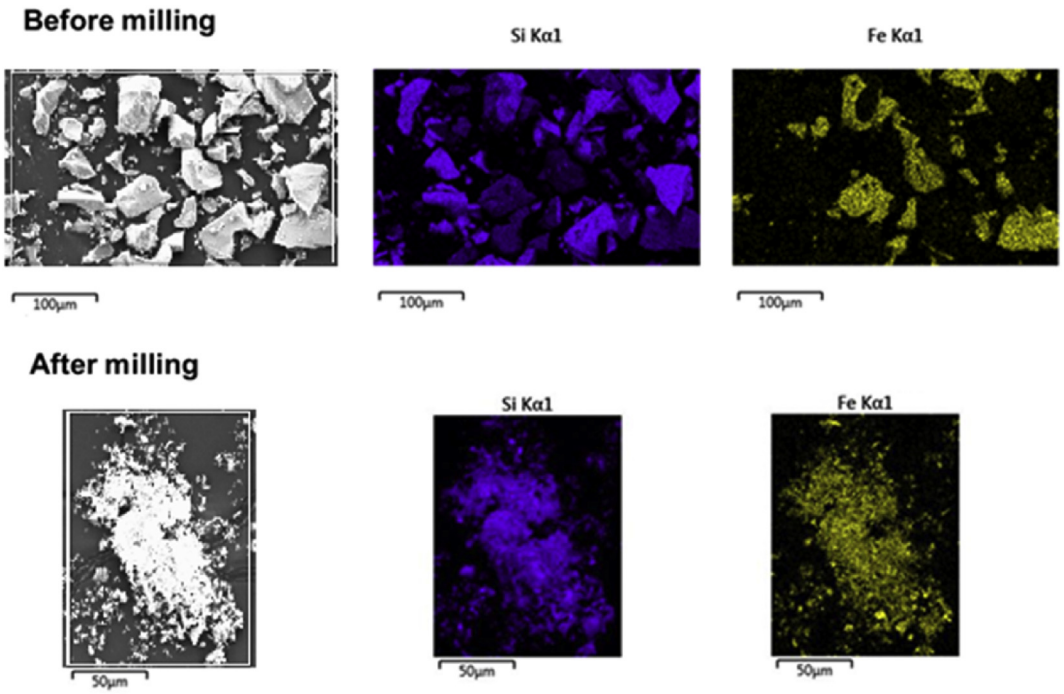

Fig. 3 – Elemental maps generated by EDX before (top) and after milling (bottom) in sequence left to right, SEM image, elemental silicon map and elemental iron map. It is clear that Si and Fe are much more homogenously distributed after milling (bottom) than they were in the as-supplied materials (top). (For interpretation of the references to colour in this figure legend, the reader is referred to the Web version of this article.)

of hydrogen generation from the as-received ferrosilicon powder [38,47], it was found that this concentration could be reduced to 0.5 M NaOH and still obtain hydrogen on a reasonable timescale once the ferrosilicon had been milled. Thus, 2 wt% NaOH was used throughout this study, since as explained in the Introduction, lower concentrations of base are inherently safer and more appropriate for the portable application of interest. A rapid increase in the reaction rate was observed in the reaction of the milled material with sodium hydroxide compared to the un-milled powders. This behaviour is entirely consistent with previous work in the area on similar materials where a decrease in particle size and increase in surface area, defects and grain boundaries increases the reaction rate.

To calculate the apparent activation energy of these powders, reactions were carried out with 2 wt% NaOH at various temperatures and the maximum rate of hydrogen generation (HGR) measured for each one (Fig. 4(a)). The natural log of the maximum rate at each temperature was then plotted against the inverse of the temperature, and the activation energy obtained from the gradient of this plot (Fig. 4(b)) [47,55,56]. An apparent activation energy of 62 kJ/mol for this process was estimated, which is some ~30 kJ/mol lower than that obtained for un-milled ferrosilicon powder. While the reduction in the particle size would be expected to lead to an increase in the reaction rate, the effect would be expected to be similar at all temperatures; in other words, the values of HGR would all change similarly, and the gradient and therefore the activation energy would be the same. Therefore, the decrease in activation energy is not ascribable to the reduction in particle size alone. Rather, the decrease in apparent activation energy after ball milling is ascribed to the removal of the inert $FeSi_2$ species from the active silicon surface and the introduction of vacancies, defects and dislocations into the surface oxide layer on the silicon particles. Breaking down the iron disilicide so the silicon is more accessible while at the same time removing any oxide formed by milling thus activates the material towards reaction. The greater number of grain boundaries within the ferrosilicon itself are then less easily passivated by oxide on the silicon due to the formation of the finely divided $FeSi_2$

To gain insight into the reaction mechanism, values of 59.3 kJ/mol and −64.4 J/K/mol were obtained for the activation enthalpy and entropy, respectively, by means of an Eyring plot (Fig. 4(c)) [47]. A negative activation entropy is associated with an associative rate determining step; this suggests that the reaction of ball milled ferrosilicon with sodium hydroxide follows a similar mechanism to that of the reaction of hydroxide and silicon, whereby the attack of hydroxide ions on silicon to form a hydrated silica complex (in other words, an associative process) is considered to be the rate determining step [57,58].

Characterisation of reaction products

The residual powders were characterised after reaction with sodium hydroxide to form hydrogen by SEM, PXRD and XPS. In agreement with previous studies on un-milled ferrosilicon powders [38], PXRD (Fig. 5(a)) showed that the silicon phase (reflections denoted by # on the figure) in the powders was completely consumed during reaction and the iron disilicide phase (reflections denoted by * in the figure) remained inert

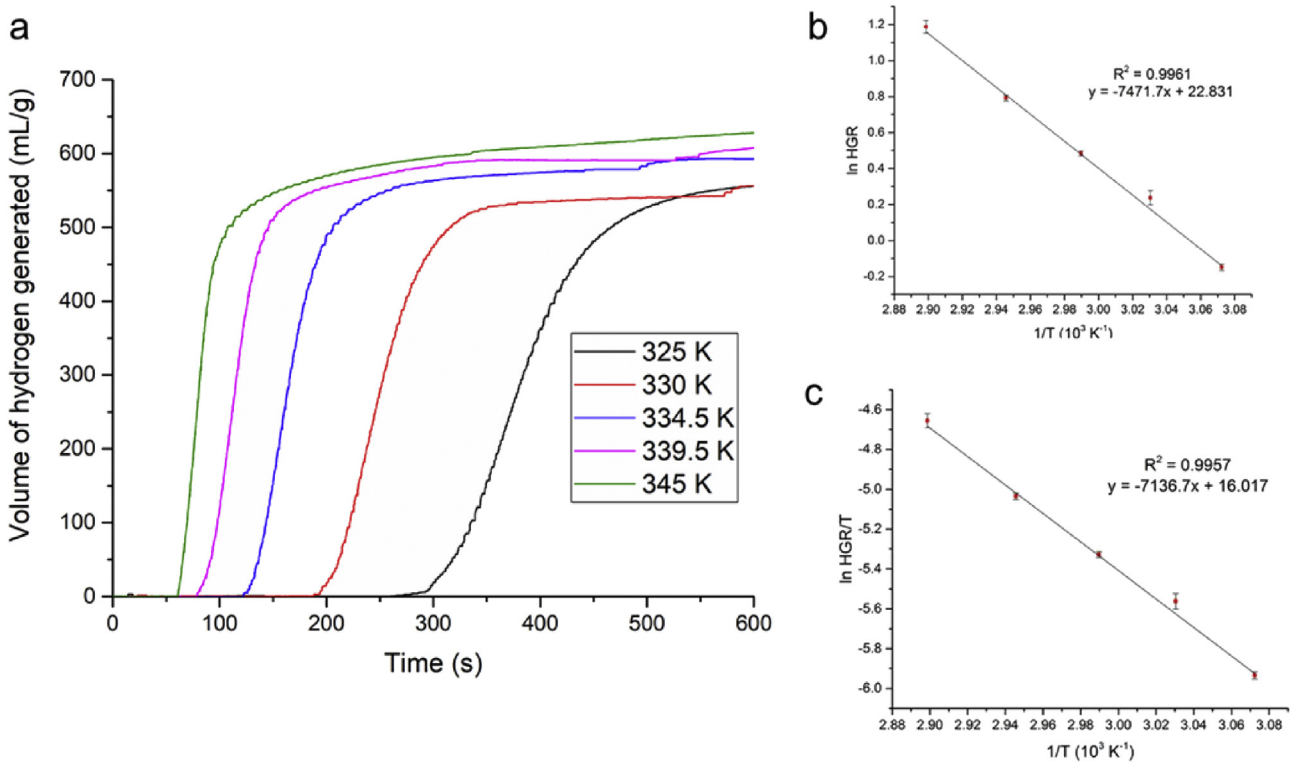

Fig. 4 – a) Hydrogen generation curves from the reaction of 0.20 g of ball-milled ferrosilicon with 5 mL of 2 wt% sodium hydroxide solution at 325, 330, 334.5, 339.5 and 345 K. b) Arrhenius plot generated from the rates of reaction extracted from the hydrogen generation curves shown in Fig. 4(a) c) Eyring plot generated from the rates of reaction extracted from the hydrogen generation curves shown in Fig. 4(a).

throughout the reaction. XPS of the Si 2p region shows that the surface oxide layer has thickened to the point that metallic silicon is no longer detectable (Fig. 5(b)). The SEM of the post-reaction powders suggests that they have a more finely structured surface than the pre-reaction powders (Fig. 5(c), (d) and (e)). These data confirm that milled ferrosilicon follows the same reaction pathway as un-milled ferrosilicon.

Investigation of the effect of additives on ferrosilicon

Having shown that ferrosilicon can be activated by ball milling, the next stage in the investigation was to see if using additives could improve the hydrogen generation properties of ferrosilicon further, in a similar way to what had been observed for silicon and aluminium. Although ball milling successfully reduced the particle size, resulting in a more rapid reaction, a lengthy induction period before hydrogen generation was detected was still maintained for ball milled ferrosilicon when reacting with a 2 wt% sodium hydroxide solution. The origin of this induction period is passivation of the ferrosilicon by surface oxide on silicon and the presence of the $FeSi_2$ protecting species. In order to further activate ferrosilicon, these effects need to be overcome and the $FeSi_2$ broken down.

Preparation and characterisation of ferrosilicon/additive composites

In order to improve the hydrogen generation properties of ferrosilicon further it was decided to investigate whether the positive effects of incorporating three best additives for silicon activation reported by Foord et al. [45,46], would also be observed for ferrosilicon. The logic that the effect should be replicated is based upon the fact that the active reagent in ferrosilicon has been shown to be silicon itself. In addition, other additives were included in the study that have been used to erode/tribologically remove surface oxide as they could theoretically undertake the same role in removing the passivating iron disilicide present in ferrosilicon. Other low toxicity, water soluble salts, sugars and polymers were also trialled on the basis of their ability to react with iron compounds such as ferrosilicon by corrosion of $FeSi_2$.

Preparation of ferrosilicon:additive composites by ball-milling
Composite powders of ferrosilicon with various additives were prepared by ball milling. A ratio of 1:0.2 was chosen for the ferrosilicon:polymer composties, and a ratio of 1:0.5 was chosen for the ferrosilicon:salt/sugar composites, based on the optimum quantities identified by Foord et al. [45,46] It was initially intended to employ elemental analysis to determine the proportion of additive (by calculation from the quantities of carbon and hydrogen) in the composite powders. The objective was to demonstrate that the theoretical rise in carbon content as different polymeric additives were used to prepare the composite powders was achieved by carrying out the analysis before and after the reaction. Since the proportion of additive was low, the calculated change in carbon content would have been between 5 and 13%. However, this

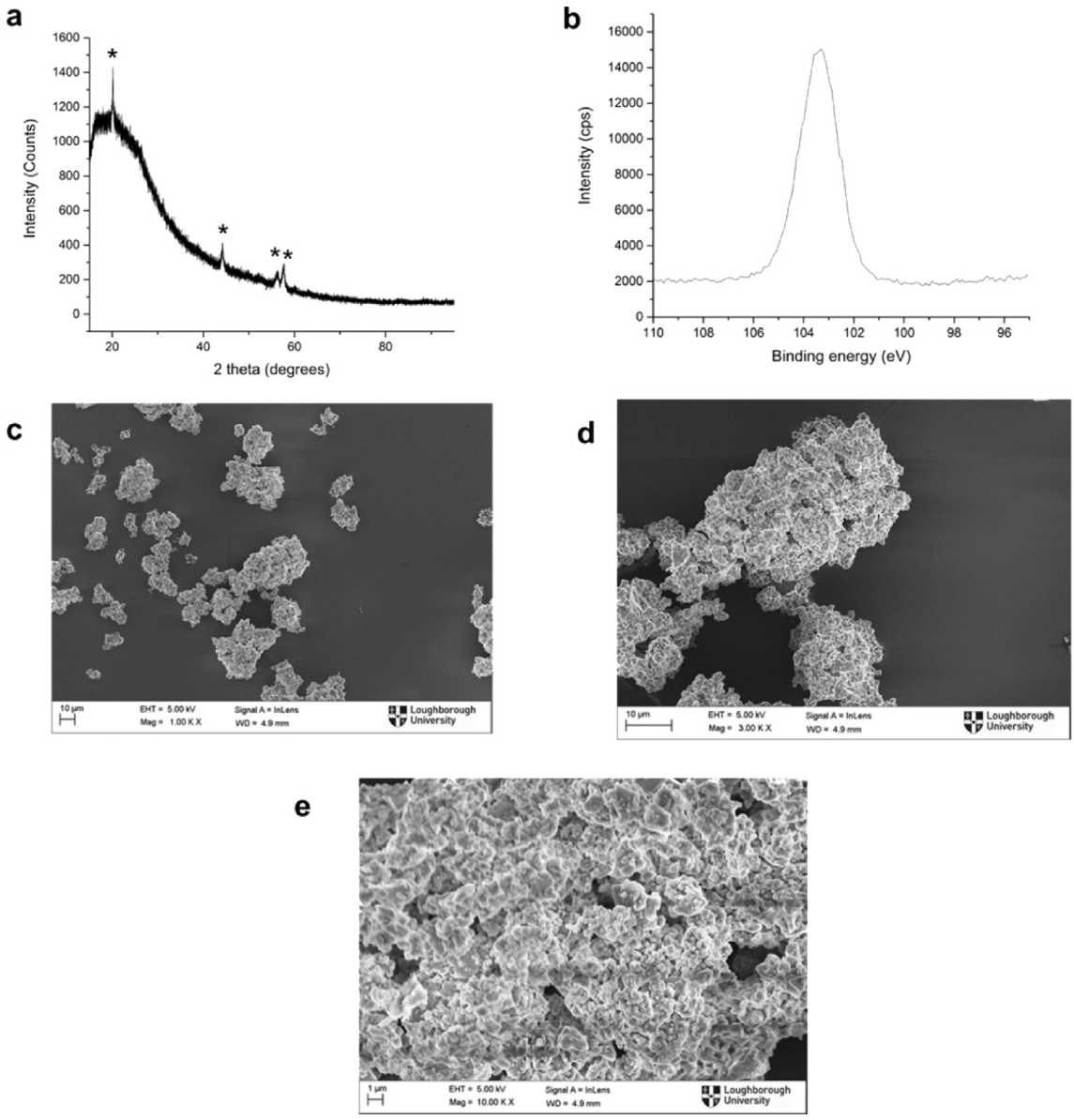

Fig. 5 – a) PXRD pattern of powder recovered after reaction of ball-milled ferrosilicon with 5 mL of 2 wt% sodium hydroxide solution at 55 °C. Reflections corresponding to iron disilicide are denoted by *. b) Si 2p region of the XPS spectra of the same powder. c), d) and e) SEM images of the same powder.

was not possible as characterisation of the industrial grade ferrosilicon powder used in this study contained highly variable amounts of carbon (0.00–1.75 wt%) which would have led to substantial uncertainty in the analysis. The source of the carbon is likely to be the result of the legacy of the coke used in the manufacturing process of ferrosilicon.

Ferrosilicon/salt composites

Three salts were initially chosen as additives; LiCl, NaCl and KCl. However, extensive investigation was limited to only the sodium and potassium salts since the lithium analogue was highly hygroscopic and the powders obtained with this additive rapidly became paste-like in consistency during the drying stage, making accurate weighing impossible.

The presence of NaCl and KCl in the composite powders was readily confirmed by PXRD (Fig. S5). Reflections at 32.02, 37.12, 53.42, 66.76, 78.78 and 90.44°2θ correspond to the (111), (200), (220), (222), (400) and (420) planes of NaCl (ICDD 00-005-0628, cubic, Fm-3m (225)), while reflections at 33.16, 47.51, 59.05, 69.37, 78.96 and 88.34°2θ correspond to the (200), (220), (222), (400), (420) and (422) planes of KCl (ICDD 00-004-0587, cubic, Fm-3m (225)). XPS analysis (Fig. S6) further confirmed the presence of K and Cl at the surface of the KCl composite and Na and Cl at the surface of the NaCl composite. TGA analysis of the composites showed minimal weight loss upon heating to 700 °C (1.75% for NaCl, 0.15% for KCl), as would be expected given the known melting points of these materials. SEM analysis (Figs. S7 and S8) showed that the particles obtained by milling with both NaCl and KCl are fairly

inhomogeneous in size, ranging from a few hundred nanometres to more than a micron in diameter.

Hydrogen generation from salt composites

The hydrogen generation properties of the composites were evaluated by reacting them with 2 wt% NaOH solution at ~55 °C and compared with a sample of ferrosilicon prepared at a similar time (Fig. 6). Addition of NaCl and KCl clearly leads to an increase in reaction rate, suggestive of a smaller particle size and/or more defects in the oxide coating, compared to ball-milled ferrosilicon itself. Such a phenomenon has also been reported for aluminium milled with salt, and this was ascribed to the inhibition of cold welding during the milling process [52]. However, ferrosilicon, given its large metallic silicon component, is likely to be somewhat less ductile and more brittle than aluminium, and thus more likely to fracture than to weld. In systems where brittle powders are milled together, it has been observed that the more brittle component becomes embedded in the less brittle component [39]; thus, milling together of ferrosilicon and either sodium or potassium chloride would lead to the formation of an intimate mixture of the two. The presence of the salt would thus inhibit agglomeration of ferrosilicon particles during the milling process, leading to more rapid reaction rates.

Contrary to the observation of Foord et al. [45,46], an extension of the time taken for the reaction to go to completion was not observed in this study. Their commentary did, however, describes the reaction of the composite with pure water; the addition of sodium hydroxide to this system is likely the primary cause of the discrepancy, as this leads to the rate of reaction being very rapid and thus it is likely that the agglomerative effect of sodium chloride in solution observed by Foord is not given sufficient time to develop in this system.

Milling with NaCl results in a substantial reduction in the induction period, whereas milling with KCl results in a far less pronounced reduction in the induction period. The length of the induction period is generally a function of the level of passivation of the powders. As KCl is hygroscopic, one possible explanation is that this would draw water into the composite as it dried, promoting the growth of the oxide layer (as it is known that the presence of moisture accelerates silicon oxide layer growth) [59–63]. However, such a scenario is not borne out by the TGA results, which show very little mass loss from the KCl composite (indeed, a greater loss was observed from the NaCl composite). Another possible explanation would be if NaCl were substantially more soluble than KCl, it would lead to the more rapid dispersion of ferrosilicon powders into the solution and thus a lowered induction period; however, the solubilities of KCl and NaCl are actually very similar (35.5 and 36.0 g/100 g H_2O, respectively, at 298 K) [28]. A final explanation relates to the ability of chloride ions to activate pitting corrosion. As there are more chloride ions per unit mass in NaCl than in KCl, the enhanced activation observed with NaCl may be due to enhanced pitting corrosion of the ferrosilicon by the greater concentration of chloride ions. None of the salt based additives effected the overall maximum hydrogen yield, suggesting that the $FeSi_2$ protector species remained unchanged by these additives. Corrosion and breakdown of the intermetallic was expected based on the presence of iron and the susceptibility of the metal to chloride-induced corrosion [64], however this was not observed.

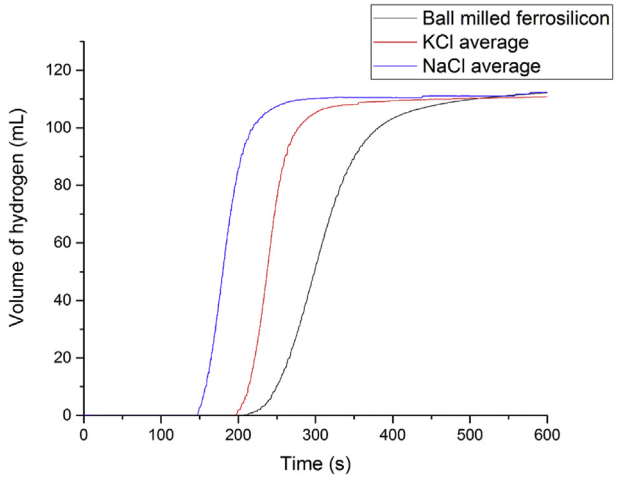

Fig. 6 – Hydrogen generation curves obtained from the reaction of ball-milled ferrosilicon, ferrosilicon-NaCl and ferrosilicon-KCl composites with 2 wt% sodium hydroxide solution at 55 °C.

Ferrosilicon/polymer composites

Polymers were divided into two subgroups: charged polymers, i.e. polyelectrolytes, and uncharged polymers. Three polyelectrolytes were chosen: sodium polyacrylate (PAA) as a weak acid, sodium polystyrene sulfonic acid (PSSS) as a strong acid and sodium polystyrene sulfonic acid co-maleic acid (PSSScoMA) as acopolymer and a strong acid). Of these, sodium polystyrene sulfonic acid is non-toxic, and the rest are irritants. Two uncharged, non-toxic polymers were also selected, namely polyethylene glycol (PEG) and polyvinylalcohol (PVA). All of these polymers are expected to be stable in an alkaline environment [65–69].

Materials characterisation of ferrosilicon/polymer composites

PXRD analysis of the composite powders showed no unexpected reflections to be present (in other words, all reflections corresponded to those observed for ferrosilicon; Fig. S9). Weight losses by TGA were broadly as expected (assuming a ratio of ferrosilicon to polymer of 1:0.2), as shown in Fig. 7. XPS analysis confirmed that the polymers and polyelectrolytes were present in the surface layers of the composite powders (Figs. S10-S12). The powders were imaged by SEM (Fig. S13); there was no remarkable difference between these powders and the ferrosilicon-salt composites.

Hydrogen generation from polymer composites

The hydrogen generation properties of the polymer composites were investigated by reaction with 5 mL of a 2 wt% sodium hydroxide solution at 55 °C (Fig. 8). The two uncharged polymers, PEG and PVA (though the alcohol groups of PVA would be expected to be partially ionised at this high a pH) and have a

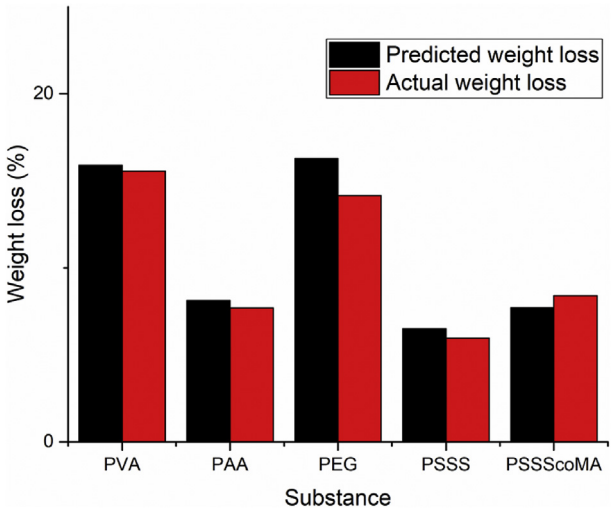

Fig. 7 – A plot of predicted and actual weight loss by TGA for PVA, PAA, PEG, PSSS and PSSScoMA.

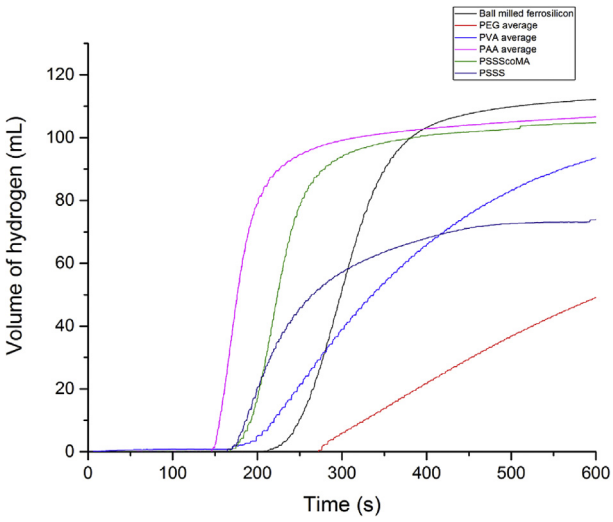

Fig. 8 – Hydrogen generation curves obtained from the reaction of ball-milled ferrosilicon-polymer composites with 2 wt% sodium hydroxide solution at 55 °C.

deleterious effect on hydrogen generation. A significant slowing in the rate of hydrogen generation and thus the yield obtained in 10 min was observed, though PVA does lead to a slight reduction in induction period at the same time. The reduction in the overall hydrogen yield indicates that $FeSi_2$ is not activated by these additives at all and that the production from the silicon component is retarded. The polyelectrolyte additives led to a significant reduction in induction period. However, the reaction with the PSSS composite resulted in a significantly lower yield of hydrogen than with ferrosilicon alone. This is ascribed to a foaming effect which was observed rapidly upon addition of the PSSS composite to the sodium hydroxide solution. The rapidly rising foam coated the side of the reaction vessel with composite powder, which, being now out of the reach of the solution, was rendered inaccessible for reaction and hydrogen generation. Addition of PSSScoMA and PAA did not result in noticeable foaming, although slightly lower than expected yields of hydrogen were obtained, perhaps indicating a slight foaming effect.

None of these polymers would be expected to undergo chemical reactions with sodium hydroxide under these conditions, so side-reactions cannot be the cause of their effects. Rather, the effects of the polymers are ascribed to steric and electrostatic influences. The uncharged polymers are likely hindering the rate of reaction due to steric effects. The goal of milling the ferrosilicon with water soluble polymers is to protect surfaces exposed during the milling process from repassivation of the surface by aerial oxidation. However, this relies on rapid dissolution of the polymer in the aqueous solution; it would seem that either the rate of dissolution of the uncharged polymers is relatively slow, which would lengthen the induction period and slow the rate by inhibiting the hydrogen generation reaction, or that the dissolution is rapid, but the increase in viscosity of the resulting solution hinders the access of sodium hydroxide to the ferrosilicon particles, thus lowering the rate of reaction.

The polyelectrolytes are added to the solution as colloidal stabilisers, as described by Foord et al. [45,46] The use of polyelectrolytes as colloidal stabilisers is well known in colloid science. The mechanism of stabilisation is thus: polyelectrolytes such as PAA (which has carboxylic acid groups), PSSS and PSSScoMA (which have sulphonic acid groups) are negatively charged in high pH basic solution, as is the surface of silicon particles (and, by extension, that of ferrosilicon, which has a silicon rich surface layer). Thus, the polyelectrolytes and the ferrosilicon particles will repel each other, more rapidly dispersing them in the solution and exposing ferrosilicon to attack by sodium hydroxide. Hence, the induction period is reduced and the rate of reaction slightly increased. The exact reason for why PAA reduces the induction period more greatly than PSSS and PSSScoMA is unclear. One explanation would be that the polyelectrolyte with the highest zeta potential would lead to the greatest increase in rate as it would represent the system in which the powders were best dispersed. Thus, the zeta potentials of the PAA and PSSScoMA composites (although it was not possible to gain a reasonable result for the PSSS composite due to it foaming during the measurement) were measured and found to be −33.1 and −67.4 mV at pH 7, respectively. This is the opposite to what would be expected. However, this may be a result of measuring the zeta potentials at pH 7 rather than the pH 14 environment in which the reactions took place (sulphonic acids are likely to be more ionised at pH 7 than carboxylic acid, resulting in a higher charge on the composite and thus a greater zeta potential; it is possible that there is a different trend in the zeta potential magnitude at pH 14 but it is impossible to measure it as the glass based cuvettes used as sample holders in the instrument would be damaged by the high causticity).

Anionic polyelectrolytes, particularly those containing a carboxylic acid, were found to be the best polymer additives for enhancing the hydrogen generation properties of ball-milled ferrosilicon powders.

Ferrosilicon/sugar composites

The third class of materials which have been investigated for their activation capability on silicon and aluminium powders

previously are sugars. Sugars are cheap and plentiful quantities which are available all over the World, so if activation of ferrosilicon for mobile applications was possible using sugars this would be impactful, since transport of ferrosilicon is much easier than other hydrogen generating materials due to higher stability. Sucrose was chosen as Foord et al. reported that sucrose was particularly effective at increasing the rate of hydrogen generation from silicon [45,46]. It was also decided to investigate the effects of milling with the components of the disaccharide sucrose, namely glucose and the highly soluble fructose, and the closely related monosaccharide mannose. A common disaccharide, lactose, was also studied to provide a comparison with sucrose.

Materials characterisation of sugar composites

Of the sugars, only lactose monohydrate is crystalline. PXRD analysis of this composite showed the reflections expected of lactose monohydrate (major reflections at 22.23, 22.73 and 23.14°2θ, ICDD 00-027-1947, monoclinic, P21 (4)), as shown in Fig. S14. The other sugars showed no unexpected reflections in their PXRD patterns (Fig. S15). Weight losses by TGA were broadly as expected assuming a 2:1 ratio of ferrosilicon:sugar in the composite powders (Fig. S16). XPS analysis of the carbon 2p and oxygen 1s regions were also indicative of the presence of the sugars in the surface layers of the composite powders (Figs. S17 and 18). The presence of the sugars in the composites was confirmed by FTIR-ATR (Fig. S19); the bands corresponding to the various sugars were also present in their respective composites. SEM analysis (Fig. S20) showed that the composite powders were inhomogeneous in particle size; no great change in particle size distribution after milling with different sugars was observed in the images.

Hydrogen generation from sugar composites

The hydrogen generation properties of the sugar composites were investigated by reaction with 5 mL of a 2 wt% sodium hydroxide solution at 55 °C (Fig. 9). Foord et al. observed that sucrose led to enhancement of the yield obtained from the reaction of silicon nanoparticles obtained by ball milling in an inert atmosphere [45]. However, we observed that sucrose led to a decrease in the reaction rate and an increase in the induction period. This is consistent with the observation of Vassilev and Russev [70], who found that sucrose reduces the activity of certain ions, including hydroxide, in solution; the decrease in rate and increase in induction period observed for the sucrose composite is consistent with the activity of the hydroxide being reduced. Fructose proved to be a particularly effective additive, slightly increasing the rate of reaction but substantially reducing the induction period. The other sugars led to less dramatic decreases in rate than sucrose, but all exhibited longer induction periods than ferrosilicon milled without an additive.

Whereas sucrose is stable under basic reaction conditions, the other sugars are not [71,72]. Glucose, for example, reacts with sodium hydroxide to form in excess of 50 different products [73–79]. Thus, it is plausible that the differences in the effects of these additives could be associated with the effect of byproducts. However, solubility is likely to be the major factor. The rationale behind milling with sugars is the same as that of milling with salts and uncharged polymers, i.e., coating the freshly exposed ferrosilicon surfaces with a water soluble protecting agent which can be rapidly removed in solution to expose the fresh, reactive surface. Thus, more water-soluble sugars ought to more greatly reduce the induction period than less soluble ones. Of these sugars, fructose is by far the most soluble (Fig. 10), and it is observed to have by far the greatest effect on the induction period.

Sucrose is the next most soluble, but, as mentioned before, seems to be a special case. Mannose is more soluble than glucose and lactose, and thus its position in the order fits; however, by this reckoning, a glucose-based composite ought to give a shorter induction period than a lactose-based one, and so clearly solubility is not the only factor affecting the

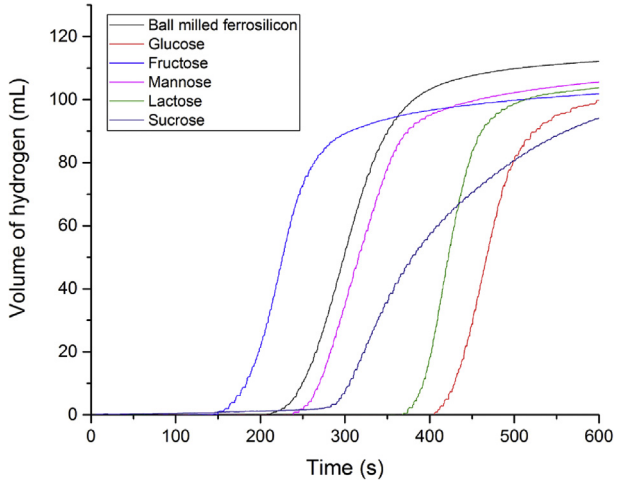

Fig. 9 – Hydrogen generation curves obtained from the reaction of ball-milled ferrosilicon-sugar composites with 2 wt% sodium hydroxide solution at 55 °C.

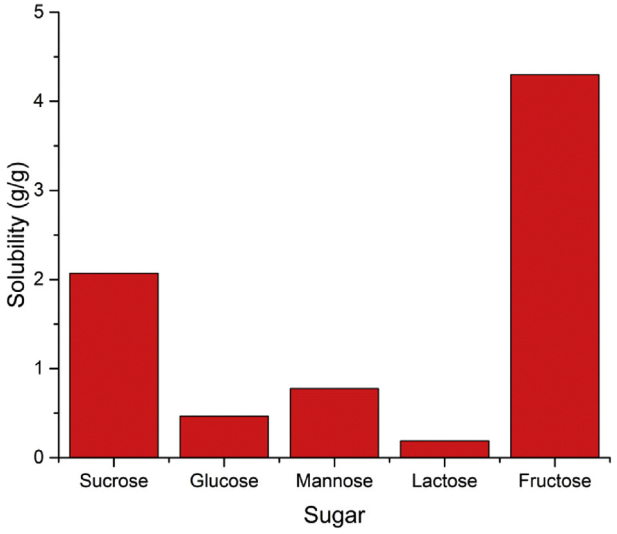

Fig. 10 – A comparison of the solubility of sucrose [80], glucose [81], mannose [82], lactose [83] and fructose [84] in water (all at 298 K apart from fructose, which was reported at 303 K).

hydrogen generation properties. It may be that glucose reacts more rapidly than does lactose with sodium hydroxide (glucose is reported to almost fully degrade in NaOH within 30 min at 80 °C) [73], which would mean that it reduced the hydroxide concentration and thus the etching power of the solution and lengthened the induction period.

Post reaction ferrosilicon/composite materials analysis

After the reaction of the composites with sodium hydroxide had taken place, the ferrosilicon powder was isolated and analysed by PXRD (Figs. S21-S23) and XPS (Figs. S24-S32). It was found that in all cases, no additive remained in the (formerly composite) powder, suggesting that the interaction of ferrosilicon and the additives was simply that of two separate components in an intimate mixture. In all cases the iron disilicide remained intact and was evidenced in the PXRD patterns, suggesting that none of the additives was successful in breaking down iron disilicide to further increase the hydrogen production by harvesting further hydrogen from the intermetallic itself. XPS did reveal iron oxide and sodium silicate at the surface of the remaindered $FeSi_2$ particles in the case of the metal salts suggesting some corrosion of the intermetallic had taken place but the bulk of the particles were unaffected as evidenced by the PXRD [38].

These experiments demonstrate why $FeSi_2$ is such an effective protector species and why it is unlikely that ferrosilicon could be used for portable device recharging, despite the very low costs of ferrosilicon compared to other hydrogen storage materials. As previously described in the introduction, ferrosilicon is a cheap industrial material consisting of a mixture of different iron/silicon species depending on the iron: silicon ratio. The ferrosilicon used in this study, is ferrosilicon 75, the theoretically best hydrogen generation material of all the ferrosilicon group of materials; the 75 refers to 75% of the material by weight being silicon and it is known to be mixture of $FeSi_2$ and Si only in a 50:50 mixture with no iron metal present. Hydrogen is generated by the silicon only and the $FeSi_2$ is a spectator species. The theoretical gravimetric storage capacity of hydrogen in silicon is 14% by weight, if surface oxidation and solubility of the metasilicate products from its reaction with water are ignored [85]. Despite the very much lower costs, due to the inactivity of $FeSi_2$ and the inability to activate it and unlock the silicon within, the storage capacity for ferrosilicon 75 is then only 3.5%. As weight is a primary factor in portable fuel cell applications for e.g recharging devices on the move, this means that any benefits seen from improving the hydrogen generation profile in terms of induction period and hydrogen output by additives to ferrosilicon is offset by the added weight of using them; since these additives have no effect on the $FeSi_2$ species at all, the maximum hydrogen yield remains associated with the silicon only.

Conclusions

Ball milling was successfully employed to activate ferrosilicon powders towards reaction with aqueous sodium hydroxide solution by improving the accessibility of the active silicon component in the 50:50, Si:$FeSi_2$ mixture. . A concentration of 2 wt% (0.5 M) sodium hydroxide could be used, with the reaction completed within 10 min. Of the tested composite materials, those formed from ferrosilicon powder and sodium chloride, potassium chloride, sodium polyacrylate, sodium polystyrene sulfonate-co-maleic acid or fructose showed reduced induction times for hydrogen generation compared to that observed for ferrosilicon alone; of these, only fructose did not lead to an increase in the maximum hydrogen generation rate. Due to its stability, lack of toxicity, abundance and low cost, sodium chloride appears to be the most promising of these additives for practical applications. Further work is required to further elucidate the mechanism of action of the additives, optimise the amounts of additives and investigate the possibility of synergistic effects from combining two or more additives with ferrosilicon in the milling process. None of the additives were successful in unlocking the silicon which is bound to iron in $FeSi_2$ to product hydrogen. The inability to access the silicon in the $FeSi_2$ means that ferrosilicon is unlikely to be practical for mobile applications, despite its cheap and easily transportable nature, as the gravimetric hydrogen storage capacity is only 3.5%. Lower weight and higher gravimetric storage capacity materials should therefore be explored for these applications.

Acknowledgements

The authors would like to thank the EPSRC and Intelligent Energy Ltd. for funding this project. PB would also like to thank the SCI for the award of a Messel Scholarship. The authors acknowledge use of the facilities and the assistance of Pat Cropper and Dr Keith Yendall in the Loughborough Materials Characterisation Centre and the assistance of Dr Jagdeep Sagu in obtaining some of the SEM images. The authors acknowledge the assistance of Harminder Cheema and Dr Sherry Ghanizadeh and thank Dr David Hutt of The Wolfson School of Mechanical, Electrical and Manufacturing Engineering for permitting us to obtain measurements using the Zetasizer Nano.

Appendix A. Supplementary data

Supplementary data to this article can be found online at https://doi.org/10.1016/j.ijhydene.2018.12.008.

REFERENCES

[1] Kim KJ, Park BH, Kim SJ, Lee Y, Bae H, Choi GM. Micro solid oxide fuel cell fabricated on porous stainless steel: a new strategy for enhanced thermal cycling ability. Sci Rep 2016;6:22443.
[2] Yao SC, Tang XD, Hsieh CC, Alyousef Y, Vladimer N, Fedder GK, Amon CH. Micro-electro-mechanical systems (MEMS)-based micro-scale direct methanol fuel cell development. Energy 2006;31:636–49.
[3] Kundu P, Dutta K. Compendium of hydrogen energy. Volume 4: hydrogen use, safety and the hydrogen economy.' chapter

6 ' 'hydrogen fuel cells for portable Applications. Woodhead Publishing; 2016. p. 111–31.
[4] Durbin DJ, Malardier-Jugroot C. Hydrogen-storage materials for mobile applications. Int J Hydrogen Energy 2013;38:14595–617.
[5] O'Malley K, Ordaz G, Adams J, Randolph K, Ahn CC, Stetson NT. Applied hydrogen storage research and development: a perspective from the US Department of Energy. J Alloy Comp 2015;645:S419–22.
[6] Stockford C, Brandon N, Irvine J, Mays T, Metcalfe I, Book D, Ekins P, Kucernak A, Molkov V, Steinberger-Wilckens R, Shah N, Dodds P, Dueso C, Samsatli S, Thompson C, 'H2FC SUPERGEN. An overview of the hydrogen and fuel cell research across the UK'. Int J Hydrogen Energy 2015;40:5534–43.
[7] Westbrook MH. The electric car: development and future of battery, hybrid and fuel cells cars. London: Institute of Electrical Engineers; 2001.
[8] O'Hayre R, Cha SW, Colella W, Prinz FB. Fuel cell fundamentals. Hobroken, New Jersey: John Wiley & Sons; 2006.
[9] Eberle U, Mueller B, von Helmolt R. Fuel cell electric vehicles and hydrogen infrastructure: status 2012. Energy Environ Sci 2012;5:8780–98.
[10] Hardman S, Chandan A, Steinberger-Wickens R. Fuel cell added value for early market applications. J Power Sources 2015;287:297–306.
[11] Xu L, Armstrong FA. Pushing the limits for enzyme-based membrane-less hydrogen fuel cells - achieving useful power and stability. RSC Adv 2015;5:3649–56.
[12] Zhang XW, Chan SH, Ho HK, Tan SC, Li MY, Li GJ, Li J, Feng ZP. Towards a smart energy network: the roles of fuel/electrolysis cells and technological perspectives. Int J Hydrogen Energy 2015;40:6866–919.
[13] Schlapbach L, Zuttel A. Hydrogen storage materials for mobile applications. Nature 2001;414:353–8.
[14] Weidenthaler C, Felderhoff M. Solid-state hydrogen storage for mobile applications: quo Vadis? Energy Environ Sci 2011;4:2495–502.
[15] Zhou L. Progress and problems in hydrogen storage methods. Renew Sustain Energy Rev 2011;15:4611–23.
[16] Shkolnikov EI, Zhuk Z, Vlaskin MS. Aluminum as energy Carrier: feasibility analysis and current technologies overview. Renew Sustain Energy Rev 2011;15:4611–23.
[17] McWhorter S, Read C, Ordaz G, Stetson N. Materials-based hydrogen storage: attributes for near-term, early market PEM fuel cells'. Curr Opin Solid State Mater Sci 2011;15:29–38.
[18] Oh S, Kim M, Eom K, Kyung J, Kim D, Cho E, Kwon H. Design of Mg-Ni alloys for fast hydrogen generation from seawater and their application in polymer electrolyte membrane fuel cells. Int J Hydrogen Energy 2016;41:5296–303.
[19] Auner N, Holl S. Silicon as energy Carrier - facts and perspectives. Energy 2006;31:1395–402.
[20] Ilyukhina AV, Ilyukin AS. Hydrogen generation from water by means of activated aluminium. Int J Hydrogen Energy 2016;37:16382–7.
[21] Soler L, Macanas J, Munoz M, Casado J. Aluminium and aluminium alloys as sources of hydrogen for fuel cell applications. Int J Hydrogen Energy 2007;32:4702–10.
[22] Martinez SS, Sanchez LA, Gallegos AAA, Sebastian PJ. Coupling of a PEM fuel cell and the hydrogen generation from aluminum waste cans. Int J Hydrogen Energy 2007;32:3159–62.
[23] Wang HZ, Leung DYC, Leung MKH. A review on hydrogen production using aluminum and aluminum alloys. Renew Sustain Energy Rev 2009;12:845–53.
[24] Fan MQ, Xu F, Sun LX. Studies on hydrogen generation characteristics of hydrolysis of the ball milling Al-based materials in pure water. Int J Hydrogen Energy 2007;32:2809–15.
[25] Rosenband V, Gany A. ' Application of activated aluminum powder for generation of hydrogen from water. Int J Hydrogen Energy 2010;35:10898–904.
[26] Hu HR, Qiao MH, Pei Y, Fan KN, Li HX, Zong BN, Zhang XX. Kinetics of hydrogen evolution in alkali leaching of rapidly quenched Ni-Al alloy. Appl. Catal. A-Gen. 2003;252:173–83.
[27] Greenwood NN, Earnshaw A. Chemistry of the elements. 1st ed. Butterworth-Heinemann; 1984. p. 380–1.
[28] Haynes WM. Handbook of chemistry and physics. 91st ed. CRC Press; 2011.
[29] Kale P, Gangal AC, Edia R, Starma P. Investigation of hydrogen storage behavior of silicon nanoparticles. Int J Hydrogen Energy 2012;37:3741–7.
[30] Mehta RN, Chakrabarty M, Parikh PA. Impact of hydrogen generated by splitting water with nano-silicon and nano-aluminum on diesel engine performance'. Int J Hydrogen Energy 2014;39:8098–105.
[31] Hu Y, Yan HY, Liu KW, Cao HM, Li W. Hydrogen production using solar grade wasted silicon. Int J Hydrogen Energy 2015;40:8633–41.
[32] Zhan CY, Chu PK, Ren D, Zin YC, Huo KF, Zou Y, Huang NK. Release of hydrogen during transformation from porous silicon to silicon oxide at normal temperature. Int J Hydrogen Energy 2011;36:4513–7.
[33] Kao TL, Huang WH, Tuan HY. Kerf loss silicon as a cost-effective, high-efficiency, and convenient energy Carrier: additive-mediated rapid hydrogen production and integrated systems for electricity generation and hydrogen storage'. J Mater Chem A 2016;33:12921–8.
[34] Erogbogbo F, Lin T, Tucciarone PM, LaJoie KM, Lai L, Patki GD, Prasad PN, Swihart MT. On-demand hydrogen generation using nanosilicon: splitting water without light. Heat, or Electricity' Nano Lett 2013;13:451–6.
[35] Goller B, Kovalev D, Sreseli O. Nanosilicon in water as a source of hydrogen: size and pH matter. Nanotechnology 2011;22:305402.
[36] Buo TV, Gray RJ, Patalsky RM. Reactivity and petrography of cokes for ferrosilicon and silicon production. Int J Coal Geol 2000;43:243–56.
[37] Weaver ER. The generation of hydrogen by the reaction between ferrosilicon and a solution of sodium hydroxide. J Ind Eng Chem 1920;12:232–40.
[38] Brack P, Dann SE, Wijayantha KGU, Adcock P, Foster S. Elucidating the process of hydrogen generation from the reaction of sodium hydroxide solution and ferrosilicon. Int J Energy Res 2017;41:1740–8.
[39] Suryanarayana C. Mechanical alloying and milling. Prog Mater Sci 2001;46:1–184.
[40] Ouyang LZ, Cao ZJ, Wang H, Hu RZ, Zhu M. Application of dielectric barrier discharge plasma-assisted milling in energy storage materials - a review. J Alloy Comp 2017;691:422–35.
[41] Huang MH, Ouyang LZ, Wang H, Liu JW, Zhu M. Hydrogen generation by hydrolysis of MgH2 and enhanced kinetics performance of ammonium chloride introducing. Int J Hydrogen Energy 2015;40:6145–50.
[42] Alinejad B, Mahmoodi K. A novel method for generating hydrogen by hydrolysis of highly activated aluminum nanoparticles in pure water. Int J Hydrogen Energy 2009;34:7934–8.
[43] Czech E, Troczynski T. Hydrogen generation through massive corrosion of deformed aluminum in water. Int J Hydrogen Energy 2010;35:1029–37.
[44] Swamy AKN, Shafirovich E. 'Conversion of aluminum foil to powders that react and burn with water. Combust Flame 2014;161:322–31.

[45] Foord JS, Hu J. Composition for hydrogen generation. WIPO; 2014. WO 2014/053799.
[46] Xu L, Ashraf S, Hu J, Edwards PP, Jones MO, Hadzifejzovic E, Foord JS. Ball-milled Si powder for the production of H-2 from water for fuel cell applications. Int J Hydrogen Energy 2016;41:12730–7.
[47] Brack P, Dann SE, Wijayantha KGU, Adcock P, Foster S. An old solution to a new problem? Hydrogen generation by the reaction of ferrosilicon with aqueous sodium hydroxide solutions' *Energy*. Sci. Eng. 2015;3:535–40.
[48] Jin Y, Zhang S, Zhu B, Tan YL, Hu XZ, Zong LW, Zhu J. Simultaneous purification and perforation of low-grade Si sources for lithium-ion battery. Anode' *Nano Lett.* 2015;15:7742–7.
[49] Zhu B, Jin Y, Tan YL, Zong LW, Hu XZ, Chen Y, Chen L, Zhang Q, Zhu J. Scalable production of Si nanoparticles directly from low grade sources for lithium-ion battery anode'. Nano Lett 2015;15:5750–4.
[50] Brack P, Dann SE, Wijayantha KGU, Adcock P, Foster S. A simple, low-cost, and robust system to measure the volume of hydrogen evolved by chemical reactions with aqueous solutions'. J. Vis. Exp.; 2016. p. e54383.
[51] Zakharov RG, Petrova SA, Zhdanov AV, Zhuchkov VI. The effect of the structure of ferrosilicon on its disintegration. Russ Metall 2014;2014:8–13.
[52] Chen X, Zhao Z, Hao M, Wang D. Research of hydrogen generation by the reaction of Al-based materials with water. J Power Sources 2013;222:188–95.
[53] Zhang DL. Processing of advanced materials using high-energy mechanical milling. Prog Mater Sci 2004;49:537–60.
[54] Huang XN, Lv CJ, Wang Y, Shen H, Chen D, Huang YX. Hydrogen generation from hydrolysis of aluminum/graphite composites with a core-shell structure. Int J Hydrogen Energy 2012;37:7457–63.
[55] Liu S, Fan M, Wang C, Huang Y, Chen D, Bai L, Shu K. Hydrogen generation by hydrolysis of Al-Li-Bi-NaCl mixture with pure water. Int J Hydrogen Energy 2012;37:1014–20.
[56] Niu F, Huang X, Gao T, Wang J, Qin L, Huang Y. Hydrogen generation from hydrolysis of ball-milled Al/C composite materials: effects of processing parameters. Energy Technol 2014;2:593–7.
[57] Seidel H, Csepregi L, Heuberger A, Baumgartel H. Anistropic etching of crystalline silicon in alkaline solutions. 1. Orientation dependence and behavior of passivation layers. J Electrochem Soc 1990;137:3612–26.
[58] Shah IA, Koekkoek JJ, van Enckevort WJP, Vlieg E. Influence of additives on alkaline etching of silicon(111). Cryst Growth Des 2009;9:4315–23.
[59] Cerofolini GF, Meda L. 'Mechanisms and kinetics of room-temperature silicon oxidation. J Non Cryst Solids 1997;216:140–7.
[60] Morita M, Ohmi T, Hasegawa E, Kawakami M, Ohwada M. ' growth of native oxide on a silicon surface. J Appl Phys 1990;68:1272–81.
[61] Miura TA, Niwano M, Shoji D, Miyamoto N. Initial stages of oxidation of hydrogen-terminated Si surface stored in air. Appl Surf Sci 1996;100:454–9.
[62] Cerofolini GF, Mascolo D, Vlad MO. A model for oxidation kinetics in air at room temperature of hydrogen-terminated (100) Si. J Appl Phys 2006;100:1–11.
[63] Salonen J, Lehto VP, Laine E. The room temperature oxidation of porous silicon. Appl Surf Sci 1997;120:191–8.
[64] Daniel P, Rapp R. Advanced corrosion science and technology. Springer; 1976. p. 55–172.
[65] Mark HF, Bialkes NM. Encyclopedia of polymer science and technology. 3rd ed., vol. 4. Interscience; 2003.
[66] Merle G, Hosseiny SS, Wessling M, Nijmeijer K. New cross-linked PVA based polymer electrolyte membranes for alkaline fuel cells. J Membr Sci 2012;409:191–9.
[67] Chen J, Spear SK, Huddleston JG, Rogers RD. 'Polyethylene glycol and solutions of polyethylene glycol as green reaction media. Green Chem 2005;7:64–82.
[68] Sagu JS, York N, Southee D, Wijayantha KGU. Printed electrodes for flexible, light-weight solid-state supercapacitors - a feasibility study. Circ World 2015;41:80–6.
[69] Li B, Lu X, Yuan J, Zhu Y, Li L. Alkaline poly(vinyl alcohol)/poly(acrylic acid) polymer electrolyte membrane for Ni-MH battery application. Ionics 2015;21:141–8.
[70] Vassilev L, Russev G. Ion activity decrease in the presence of sucrose. Biochim Biophys Acta - Gen Subj 1981;675:214–6.
[71] de Bruijn JM, Kieboom APG, van Bekkum H. Alkaline degradation of monosaccharides 5. Kinetics of the alkaline isomerization and degradation of monosaccharides. Recl Trav Chim Pays-Bas 1987;106:35–43.
[72] Dendene K, Guihard L, Nicolas S, Bariou B. Kinetics of lactose isomerization to lactulose in an alkaline medium. J Chem Tech Biotechnol 1994;61:37–42.
[73] Marianou A, Michailof CM, Pineda A, Iliopoulou EF, Triantafyllidis KS, Lappas A. Glucose to fructose isomerization in aqueous media over homogeneous and heterogeneous catalysts. ChemCatChem 2016:1100–10.
[74] Moulik SP, Basu D, Bhattacharya PK. Effects of various conditions on alkaline degradation of D-fructose and D-glucose. Carbohydr Res 1978;63:165–72.
[75] De Wilt HGJ, Kuster BFM. Oxidation of D-glucose and D-frutose with oxygen in aqueous alkaline solution 1 integral reaction scheme. Carbohydr Res 1971;19:5–15.
[76] De Wilt HGJ, Lindhout I. Oxidation of D-glucose and D-frutose with oxygen in aqueous alkaline solution 2 overall KineticsKinetic approach to product distribution. Carbohydr Res 1971;23:333–41.
[77] De Wilt HGJ, Kuster BFM. Oxidation of D-glucose and D-frutose with oxygen in aqueous alkaline solution 3 kinetic approach to product distribution. Carbohydr Res 1972;23:343–8.
[78] Sowden JC, Schaffer R. The reaction of D-glucose, D-mannose and D-fructose in 0.035N sodium hydroxide at 35 degrees. J Am Chem Soc 1952;74:499–504.
[79] Yang BY, Montgomery R. Alkaline degradation of glucose: effect of initial concentration of reactants. Carbohydr Res 1996;280:27–45.
[80] Asadi M. Beet-sugar handbook. Hoboken, New Jersey: John Wiley & Sons; 2007.
[81] Zhang D, Montañés F, Srinivas K, Fornari T, Ibáñez E, King JW. Measurement and correlation of the solubility of carbohydrates in subcritical water. Ind Eng Chem Res 2010;49:6691–8.
[82] Gong X, Wang C, Zhang L, Qu H. Measurement and correlation of the solubility of carbohydrates in subcritical water. J Chem Eng Data 2012;57:3264–9.
[83] Machado JJB, Coutinho JAP, Macedo EA. Solid-liquid equilibrium of alpha-lactose in ethanol/water. Fluid Phase Equil 2000;173:121–34.
[84] Flood AE, Puagsa S. 'Refractive index, viscosity, and solubility at 30 degrees C, and density at 25 degrees C for the system fructose plus glucose plus ethanol plus water. J Chem Eng Data 2000;45:902–7.
[85] Brack P, Dann SE, Wijayantha KGU, Adcock P, Foster S. An assessment of the viability of hydrogen generation from the reaction of silicon powder and sodium hydroxide solution for portable applications. Int J Energy Res 2017;41:220–8.